Interelectronic-interaction effect on the transition probability in high-Z He-like ions

P. Indelicato,[1] V. M. Shabaev,[2] and A. V. Volotka[2]

[1]*Laboratoire Kastler-Brossel, École Normale Supérieure et Université Pierre et Marie Curie, Case 74, 4, place Jussieu, 75252 Paris CEDEX 05, France*

[2]*Department of Physics, St. Petersburg State University, Oulianovskaya 1, Petrodvorets, St. Petersburg 198504, Russia*

(Received 1 December 2003; published 10 June 2004)

The interelectronic-interaction effect on the transition probabilities in high-Z He-like ions is investigated within a systematic quantum electrodynamic approach. The calculation formulas for the interelectronic-interaction corrections of first order in $1/Z$ are derived using the two-time Green-function method. These formulas are employed for numerical evaluations of the magnetic transition probabilities in heliumlike ions. The results of the calculations are compared with experimental values and previous calculations.

I. INTRODUCTION

During the last few years, transition probabilities in heliumlike ions were calculated by a number of authors [1–4]. In these calculations, the interelectronic-interaction effects on the transition probabilities were accounted for by employing the relativistic many-body perturbation theory (RMBPT) [1,2,4] and the multiconfiguration Dirac-Fock (MCDF) method [3]. Since these methods are based on using the Coulomb-Breit Hamiltonian, they have to deal with separate treatment of the positive- and negative-energy state contributions. As was first indicated in Ref. [3], the contribution from the negative-continuum contribution is very sensitive to the choice of the one-electron model potential, which is used as the starting point of any RMBPT or MCDF calculation. In particular, using a standard Dirac-Fock approximation, in Ref. [3] it has been demonstrated that to achieve the agreement between theory and experiment for the magnetic dipole transition $2\,^3S_1 \rightarrow 1\,^1S_0$ it is necessary to take into account both correlation and negative-continuum effects. This statement is closely related to a problem of significant numerical cancellations that may occur in low-Z systems, if an improper one-electron approximation is used. For a rigorous QED approach for low-Z systems and corresponding calculations we refer to Refs. [5,6].

The main goal of the present paper is to perform a complete QED calculation of the interelectronic-interaction correction of first order in $1/Z$ to the magnetic transition probabilities in high-Z He-like ions. To derive the calculation formulas for these corrections from the first principles of QED we use the two-time Green-function method developed in Refs. [7–9] and described in detail in Ref. [10]. In Sec. II, we formulate the basic equations of this method for the case of nondegenerate states and apply it for the derivation of the desired formulas. The numerical results for the transitions $2\,^3S_1 \rightarrow 1\,^1S_0$, $2\,^3P_2 \rightarrow 1\,^1S_0$, and $3\,^3S_1 \rightarrow 2\,^3S_1$ are presented in Sec. III. Both Feynman and Coulomb gauges are used for the photon propagator to demonstrate the gauge independence of the final results. The results of the calculations are compared with previous theoretical results and with experiment.

The relativistic units ($\hbar = c = 1$) and the Heaviside charge unit [$\alpha = e^2/(4\pi), e < 0$] are used in the paper.

II. BASIC FORMULAS

We consider the transition of a high-Z two-electron ion from an initial state a to a final state b with the emission of a photon with momentum $\mathbf{k}_f$ and polarization $\boldsymbol{\epsilon}_f$. The transition probability is given as

$$dW = 2\pi |\tau_{\gamma_f,b;a}|^2 \delta(E_b + k_f^0 - E_a) d\mathbf{k}_f, \quad (1)$$

where $\tau_{\gamma_f,b;a}$ is the transition amplitude which is connected with the S-matrix element by

$$\langle \mathbf{k}_f, \boldsymbol{\epsilon}_f; b | S | a \rangle = 2\pi i \tau_{\gamma_f,b;a} \delta(\varepsilon_b + k_f^0 - \varepsilon_a), \quad (2)$$

and $k_f^0 \equiv |\mathbf{k}_f|$.

We assume that in zeroth (one-electron) approximation the initial and final states of the ion are described by one-determinant wave functions

$$u_a(\mathbf{x}_1, \mathbf{x}_2) = \frac{1}{\sqrt{2}} \sum_P (-1)^P \psi_{Pa_1}(\mathbf{x}_1) \psi_{Pa_2}(\mathbf{x}_2), \quad (3)$$

$$u_b(\mathbf{x}_1, \mathbf{x}_2) = \frac{1}{\sqrt{2}} \sum_P (-1)^P \psi_{Pb_1}(\mathbf{x}_1) \psi_{Pb_2}(\mathbf{x}_2). \quad (4)$$

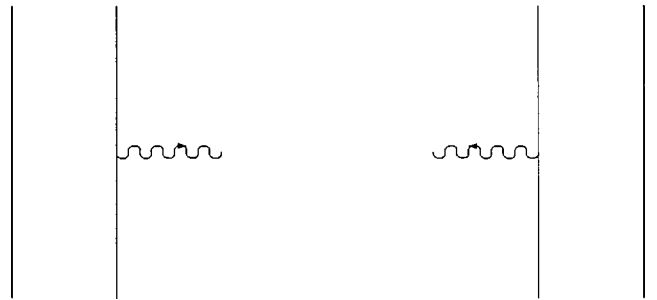To describe the process under consideration we introduce the Green function $g_{\gamma_f,b;a}(E', E)$ by

FIG. 1. The photon emission by a heliumlike ion in zeroth-order approximation.

$$g_{\gamma_f,b;a}(E',E)\delta(E'+k^0-E)=\frac{1}{2!}\int_{-\infty}^{\infty}dp_1^0dp_2^0dp_1'^0dp_2'^0\delta(E-p_1^0-p_2^0)\delta(E'-p_1'^0-p_2'^0)$$

$$\times\int d\mathbf{x}_1d\mathbf{x}_2d\mathbf{x}_1'd\mathbf{x}_2'u_b^\dagger(\mathbf{x}_1',\mathbf{x}_2')G_{\gamma_f}((p_1'^0,\mathbf{x}_1'),(p_2'^0,\mathbf{x}_2');k^0;(p_1^0,\mathbf{x}_1),(p_2^0,\mathbf{x}_2))\gamma_1^0\gamma_2^0u_a(\mathbf{x}_1,\mathbf{x}_2),\qquad(5)$$

where

$$G_{\gamma_f}((p_1'^0,\mathbf{x}_1'),(p_2'^0,\mathbf{x}_2');k^0;(p_1^0,\mathbf{x}_1),(p_2^0,\mathbf{x}_2))=\frac{2\pi}{i}\frac{1}{(2\pi)^5}\int_{-\infty}^{\infty}dx_1^0dx_2^0dx_1'^0dx_2'^0\int d^4y\,\exp(ip_1'^0x_1'^0$$

$$+ip_2'^0x_2'^0-ip_1^0x_1^0-ip_2^0x_2^0+ik^0y^0)A_f^{\nu*}(\mathbf{y})\langle0|T\psi(x_1')\psi(x_2')j_\nu(y)\bar\psi(x_2)\bar\psi(x_1)|0\rangle\quad(6)$$

is the Fourier transform of the four-time Green function describing the process, $\psi(\mathbf{x})$ is the electron-positron field operator in the Heisenberg representation, and

$$A_f^\nu(\mathbf{x})=\frac{\epsilon_f^\nu\exp(i\mathbf{k}_f\cdot\mathbf{x})}{\sqrt{2k_f^0(2\pi)^3}}\qquad(7)$$

is the wave function of the emitted photon. The transition amplitude $S_{\gamma_f,b;a}\equiv\langle\mathbf{k}_f,\boldsymbol{\epsilon}_f;b|S|a\rangle$ is calculated by Refs. [7,8,10]

$$S_{\gamma_f,b;a}=Z_3^{-1/2}\delta(E_b+k_f^0-E_a)\oint_{\Gamma_b}dE'\oint_{\Gamma_a}dEg_{\gamma_f,b;a}(E',E)\left[\frac{1}{2\pi i}\oint_{\Gamma_b}dEg_{bb}(E)\right]^{-1/2}\left[\frac{1}{2\pi i}\oint_{\Gamma_a}dEg_{aa}(E)\right]^{-1/2}.\qquad(8)$$

Here $g_{aa}(E)$ is defined by

$$g_{aa}(E)\delta(E'-E)=\frac{2\pi}{i}\frac{1}{2!}\int_{-\infty}^{\infty}dp_1^0dp_2^0dp_1'^0dp_2'^0\delta(E-p_1^0-p_2^0)\delta(E'-p_1'^0-p_2'^0)$$

$$\times\int d\mathbf{x}_1d\mathbf{x}_2d\mathbf{x}_1'd\mathbf{x}_2'u_a^\dagger(\mathbf{x}_1',\mathbf{x}_2')G((p_1'^0,\mathbf{x}_1'),(p_2'^0,\mathbf{x}_2');(p_1^0,\mathbf{x}_1),(p_2^0,\mathbf{x}_2))\gamma_1^0\gamma_2^0u_a(\mathbf{x}_1,\mathbf{x}_2),\qquad(9)$$

where

$$G((p_1'^0,\mathbf{x}_1'),(p_2'^0,\mathbf{x}_2');(p_1^0,\mathbf{x}_1),(p_2^0,\mathbf{x}_2))=\frac{1}{(2\pi)^4}\int_{-\infty}^{\infty}dx_1^0dx_2^0dx_1'^0dx_2'^0\exp(ip_1'^0x_1'^0+ip_2'^0x_2'^0-ip_1^0x_1^0-ip_2^0x_2^0)$$

$$\times\langle0|T\psi(x_1')\psi(x_2')\bar\psi(x_2)\bar\psi(x_1)|0\rangle\qquad(10)$$

is the Fourier transform of the four-time Green function describing the ion; $g_{bb}(E)$ is defined by a similar equation. The contours Γ_a and Γ_b surround the poles corresponding to the initial and final levels and keep outside all other singularities of the Green functions. It is assumed that they are oriented counterclockwise. The Green functions G and G_{γ_f} are constructed by perturbation theory after the transition to the interaction representation and using Wick's theorem. The Feynman rules for G and G_{γ_f} are given, e.g., in Ref. [10].

Below we consider the transition probability in high-Z He-like ion to zeroth and first order in $1/Z$.

A. Zeroth-order approximation

To zeroth order in $1/Z$ the transition amplitude is described by the diagrams shown in Fig. 1. Formula (8) gives

$$S_{\gamma_f,b;a}^{(0)}=\delta(E_b+k_f^0-E_a)\oint_{\Gamma_b}dE'\oint_{\Gamma_a}dEg_{\gamma_f,b;a}^{(0)}(E',E),\qquad(11)$$

where the superscript indicates the order in $1/Z$. According to definition (5) and the Feynman rules for G_{γ_f} [10], we have

$$g^{(0)}_{\gamma_f,b;a}(E',E)\delta(E'+k^0-E)=\sum_P(-1)^P\int_{-\infty}^{\infty}dp_1^0dp_2^0dp_1'^0dp_2'^0\delta(E-p_1^0-p_2^0)\delta(E'-p_1'^0-p_2'^0)$$

$$\times\left\{\langle Pb_1|\frac{i}{2\pi}\sum_{n_1}\frac{|n_1\rangle\langle n_1|}{p_1'^0-\varepsilon_{n_1}(1-i0)}\frac{2\pi}{i}e\alpha_\mu\delta(p_1'^0+k^0-p_1^0)A_f^{\mu*}\frac{i}{2\pi}\sum_{n_2}\frac{|n_2\rangle\langle n_2|}{p_1^0-\varepsilon_{n_2}(1-i0)}|a_1\rangle\right.$$

$$\times\langle Pb_2|\frac{i}{2\pi}\sum_{n_3}\frac{|n_3\rangle\langle n_3|}{p_2^0-\varepsilon_{n_3}(1-i0)}|a_2\rangle\delta(p_2'^0-p_2^0)+\langle Pb_1|\frac{i}{2\pi}\sum_{n_1}\frac{|n_1\rangle\langle n_1|}{p_1^0-\varepsilon_{n_1}(1-i0)}|a_1\rangle\delta(p_1'^0-p_1^0)$$

$$\left.\times\langle Pb_2|\frac{i}{2\pi}\sum_{n_2}\frac{|n_2\rangle\langle n_2|}{p_2'^0-\varepsilon_{n_2}(1-i0)}\frac{2\pi}{i}e\alpha_\mu\delta(p_2'^0+k^0-p_2^0)A_f^{\mu*}\frac{i}{2\pi}\sum_{n_3}\frac{|n_3\rangle\langle n_3|}{p_2^0-\varepsilon_{n_3}(1-i0)}|a_2\rangle\right\},\quad(12)$$

where $\alpha^\mu=\gamma^0\gamma^\mu=(1,\boldsymbol{\alpha})$. One obtains

$$g^{(0)}_{\gamma_f,b;a}(E',E)=\left(\frac{i}{2\pi}\right)^2\int_{-\infty}^{\infty}dp_1^0\frac{1}{p_1^0-(E-E')-\varepsilon_{b_1}+i0}\langle b_1|e\alpha_\mu A_f^{\mu*}|a_1\rangle\frac{1}{p_1^0-\varepsilon_{a_1}+i0}\frac{\delta_{a_2b_2}}{E-p_1^0-\varepsilon_{a_2}+i0}$$

$$+\left(\frac{i}{2\pi}\right)^2\int_{-\infty}^{\infty}dp_2^0\frac{1}{p_2^0-(E-E')-\varepsilon_{b_2}+i0}\langle b_2|e\alpha_\mu A_f^{\mu*}|a_2\rangle\frac{1}{p_2^0-\varepsilon_{a_2}+i0}\frac{\delta_{a_1b_1}}{E-p_2^0-\varepsilon_{a_1}+i0}\quad(13)$$

$$=\frac{i}{2\pi}\frac{1}{E'-E_b^{(0)}}[\langle b_1|e\alpha_\mu A_f^{\mu*}|a_1\rangle\delta_{a_2b_2}+\langle b_2|e\alpha_\mu A_f^{\mu*}|a_2\rangle\delta_{a_1b_1}]\frac{1}{E-E_a^{(0)}},\quad(14)$$

where $E_a^{(0)}=\varepsilon_{a_1}+\varepsilon_{a_2}$ and $E_b^{(0)}=\varepsilon_{b_1}+\varepsilon_{b_2}$. Substituting this expression into Eq. (11) and integrating over E and E' we find

$$S^{(0)}_{\gamma_f,b;a}=-2\pi i\delta(E_b+k_f^0-E_a)[\langle b_1|e\alpha_\mu A_f^{\mu*}|a_1\rangle\delta_{a_2b_2}+\langle b_2|e\alpha_\mu A_f^{\mu*}|a_2\rangle\delta_{a_1b_1}]\quad(15)$$

or, according to definition (2),

$$\tau^{(0)}_{\gamma_f,b;a}=-[\langle b_1|e\alpha_\mu A_f^{\mu*}|a_1\rangle\delta_{a_2b_2}+\langle b_2|e\alpha_\mu A_f^{\mu*}|a_2\rangle\delta_{a_1b_1}].\quad(16)$$

The corresponding transition probability is

$$dW^{(0)}=2\pi|\tau^{(0)}_{\gamma_f,b;a}|^2\delta(E_b+k_f^0-E_a)d\mathbf{k}_f.\quad(17)$$

B. Interelectronic-interaction corrections of first order in $1/Z$

The interelectronic-interaction corrections to the transition amplitude of first order in $1/Z$ are defined by diagrams shown in Figs. 2(a) and 2(b). Formula (8) yields, in the order under consideration,

$$S^{(1)}_{\gamma_f,b;a}=\delta(E_b+k_f^0-E_a)\left[\oint_{\Gamma_b}dE'\oint_{\Gamma_a}dEg^{(1)}_{\gamma_f,b;a}(E',E)-\frac{1}{2}\oint_{\Gamma_b}dE'\oint_{\Gamma_a}dEg^{(0)}_{\gamma_f,b;a}(E',E)\right.$$

$$\left.\times\left(\frac{1}{2\pi i}\oint_{\Gamma_a}dEg^{(1)}_{aa}(E)+\frac{1}{2\pi i}\oint_{\Gamma_b}dEg^{(1)}_{bb}(E)\right)\right],\quad(18)$$

where $g^{(1)}_{aa}(E)$ and $g^{(1)}_{bb}(E)$ are defined by the first-order interelectronic-interaction diagram (Fig. 3). Let us consider first the contribution of the diagrams shown in Fig. 2(a). According to the definition (5) and the Feynman rules for G_{γ_f} [10], we have

$$g^{(1a)}_{\gamma_f,b;a}(E',E)\delta(E'+k^0-E)=\sum_P(-1)^P\int_{-\infty}^{\infty}dp_1^0dp_2^0dp_1'^0dp_2'^0\delta(E-p_1^0-p_2^0)\delta(E'-p_1'^0-p_2'^0)$$

$$\times\left(\frac{i}{2\pi}\right)^3\int_{-\infty}^{\infty}dq^0d\omega\left\{\frac{1}{p_1'^0-\varepsilon_{Pb_1}+i0}\sum_n\langle Pb_1|e\alpha_\mu A_f^{\mu*}|n\rangle\frac{1}{q^0-\varepsilon_n(1-i0)}\right.$$

$$\times\langle nPb_2|I(\omega)|a_1a_2\rangle\frac{1}{p_1^0-\varepsilon_{a_1}+i0}\frac{1}{p_2'^0-\varepsilon_{Pb_2}+i0}\frac{1}{p_2^0-\varepsilon_{a_2}+i0}\delta(p_1^0-\omega-q^0)$$

$$\times\delta(q^0-k^0-p_1'^0)\delta(p_2^0+\omega-p_2'^0)+\frac{1}{p_2'^0-\varepsilon_{Pb_2}+i0}\sum_n\langle Pb_2|e\alpha_\mu A_f^{\mu*}|n\rangle$$

$$\times \frac{1}{q^0 - \varepsilon_n(1-i0)} \langle Pb_1 n|I(\omega)|a_1 a_2\rangle \frac{1}{p_2^0 - \varepsilon_{a_2} + i0} \frac{1}{p_1'^0 - \varepsilon_{Pb_1} + i0} \frac{1}{p_1^0 - \varepsilon_{a_1} + i0}$$

$$\times \delta(p_2^0 - \omega - q^0)\delta(q^0 - k^0 - p_2'^0)\delta(p_1^0 + \omega - p_1'^0)\Bigg\}, \tag{19}$$

where $I(\omega) = e^2 \alpha^\mu \alpha^\nu D_{\mu\nu}(\omega)$ and

$$D_{\rho\sigma}(\omega, \mathbf{x} - \mathbf{y}) = -g_{\rho\sigma} \int \frac{d\mathbf{k}}{(2\pi)^3} \frac{\exp[i\mathbf{k}\cdot(\mathbf{x} - \mathbf{y})]}{\omega^2 - \mathbf{k}^2 + i0} \tag{20}$$

is the photon propagator in the Feynman gauge. One finds

$$g_{\gamma_f,b;a}^{(1a)}(E',E) = \left(\frac{i}{2\pi}\right)^3 \sum_P (-1)^P \sum_n \int_{-\infty}^{\infty} dp_2^0 dp_2'^0 \frac{1}{p_2'^0 - \varepsilon_{Pb_2} + i0} \frac{1}{E' - p_2'^0 - \varepsilon_{Pb_1} + i0} \frac{1}{p_2^0 - \varepsilon_{a_2} + i0} \frac{1}{E - p_2^0 - \varepsilon_{a_1} + i0}$$

$$\times \langle Pb_1|e\alpha_\mu A_f^{\mu*}|n\rangle \frac{1}{E - p_2'^0 - \varepsilon_n(1-i0)} \langle n Pb_2|I(p_2'^0 - p_2^0)|a_1 a_2\rangle + \left(\frac{i}{2\pi}\right)^3$$

$$\times \sum_P (-1)^P \sum_n \int_{-\infty}^{\infty} dp_1^0 dp_1'^0 \frac{1}{p_1'^0 - \varepsilon_{Pb_1} + i0} \frac{1}{E' - p_1'^0 - \varepsilon_{Pb_2} + i0} \frac{1}{p_1^0 - \varepsilon_{a_1} + i0} \frac{1}{E - p_1^0 - \varepsilon_{a_2} + i0}$$

$$\times \langle Pb_2|e\alpha_\mu A_f^{\mu*}|n\rangle \frac{1}{E - p_1'^0 - \varepsilon_n(1-i0)} \langle Pb_1 n|I(p_1'^0 - p_1^0)|a_1 a_2\rangle. \tag{21}$$

The expression (21) is conveniently divided into *irreducible* and *reducible* parts. The reducible part is the one with $\varepsilon_{Pb_2} + \varepsilon_n = E_a^{(0)}$ in first term and with $\varepsilon_{Pb_1} + \varepsilon_n = E_a^{(0)}$ in second term. The irreducible part is the reminder. Using the identities

$$\frac{1}{p_1^0 - \varepsilon_{a_1} + i0} \frac{1}{E - p_1^0 - \varepsilon_{a_2} + i0} = \frac{1}{E - E_a^{(0)}}\left(\frac{1}{p_1^0 - \varepsilon_{a_1} + i0} + \frac{1}{E - p_1^0 - \varepsilon_{a_2} + i0}\right), \tag{22}$$

$$\frac{1}{p_1'^0 - \varepsilon_{Pb_1} + i0} \frac{1}{E' - p_1'^0 - \varepsilon_{Pb_2} + i0} = \frac{1}{E' - E_b^{(0)}}\left(\frac{1}{p_1'^0 - \varepsilon_{Pb_1} + i0} + \frac{1}{E' - p_1'^0 - \varepsilon_{Pb_2} + i0}\right), \tag{23}$$

we obtain for the irreducible part

$$\tau_{\gamma_f,b;a}^{(1a,\mathrm{irred})} = \frac{1}{2\pi i}\oint_{\Gamma_b} dE' \oint_{\Gamma_a} dE\ g_{\gamma_f,b;a}^{(1a,\mathrm{irred})}(E',E)$$

$$= \frac{1}{2\pi i}\oint_{\Gamma_b} dE' \oint_{\Gamma_a} dE \frac{1}{E' - E_b^{(0)}} \frac{1}{E - E_a^{(0)}}\Bigg\{ \sum_P (-1)^P \left(\frac{i}{2\pi}\right)^3 \int_{-\infty}^{\infty} dp_2^0 dp_2'^0 \left(\frac{1}{p_2'^0 - \varepsilon_{Pb_2} + i0} + \frac{1}{E' - p_2'^0 - \varepsilon_{Pb_1} + i0}\right)$$

$$\times \left(\frac{1}{p_2^0 - \varepsilon_{a_2} + i0} + \frac{1}{E - p_2^0 - \varepsilon_{a_1} + i0}\right) \sum_n^{\varepsilon_{Pb_2}+\varepsilon_n \neq E_a^{(0)}} \langle Pb_1|e\alpha_\mu A_f^{\mu*}|n\rangle \frac{1}{E - p_2'^0 - \varepsilon_n(1-i0)}\langle n Pb_2|I(p_2'^0 - p_2^0)|a_1 a_2\rangle$$

$$+ \sum_P (-1)^P \left(\frac{i}{2\pi}\right)^3 \int_{-\infty}^{\infty} dp_1^0 dp_1'^0 \left(\frac{1}{p_1'^0 - \varepsilon_{Pb_1} + i0} + \frac{1}{E' - p_1'^0 - \varepsilon_{Pb_2} + i0}\right)\left(\frac{1}{p_1^0 - \varepsilon_{a_1} + i0}\right.$$

$$\left.+ \frac{1}{E - p_1^0 - \varepsilon_{a_2} + i0}\right) \sum_n^{\varepsilon_{Pb_1}+\varepsilon_n \neq E_a^{(0)}} \langle Pb_2|e\alpha_\mu A_f^{\mu*}|n\rangle \frac{1}{E - p_1'^0 - \varepsilon_n(1-i0)}\langle Pb_1 n|I(p_1'^0 - p_1^0)|a_1 a_2\rangle \Bigg\}. \tag{24}$$

The expression in the curly braces of Eq. (24) is a regular function of E or E' when $E \approx E_a^{(0)}$ and $E' \approx E_b^{(0)}$ (see Ref. [10] for details). Calculating the residues and taking into account the identity,

$$\frac{i}{2\pi}\left(\frac{1}{x + i0} + \frac{1}{-x + i0}\right) = \delta(x), \tag{25}$$

we find

$$\tau_{\gamma_f,b;a}^{(1a,\text{irred})} = -\sum_P (-1)^P \left\{ \sum_n^{\varepsilon_{Pb_2}+\varepsilon_n \neq E_a^{(0)}} \langle Pb_1|e\alpha_\mu A_f^{\mu*}|n\rangle \frac{1}{E_a^{(0)}-\varepsilon_{Pb_2}-\varepsilon_n} \langle nPb_2|I(\varepsilon_{Pb_2}-\varepsilon_{a_2})|a_1a_2\rangle \right.$$
$$\left. + \sum_n^{\varepsilon_{Pb_1}+\varepsilon_n \neq E_a^{(0)}} \langle Pb_2|e\alpha_\mu A_f^{\mu*}|n\rangle \frac{1}{E_a^{(0)}-\varepsilon_{Pb_1}-\varepsilon_n} \langle Pb_1n|I(\varepsilon_{Pb_1}-\varepsilon_{a_1})|a_1a_2\rangle \right\}. \tag{26}$$

A similar calculation of the irreducible part of the diagrams shown in Fig. 2(b) yields

$$\tau_{\gamma_f,b;a}^{(1b,\text{irred})} = -\sum_P (-1)^P \left\{ \sum_n^{\varepsilon_{a_2}+\varepsilon_n \neq E_b^{(0)}} \langle Pb_1Pb_2|I(\varepsilon_{Pb_2}-\varepsilon_{a_2})|na_2\rangle \frac{1}{E_b^{(0)}-\varepsilon_{a_2}-\varepsilon_n} \langle n|e\alpha_\mu A_f^{\mu*}|a_1\rangle \right.$$
$$\left. + \sum_n^{\varepsilon_{a_1}+\varepsilon_n \neq E_b^{(0)}} \langle Pb_1Pb_2|I(\varepsilon_{Pb_1}-\varepsilon_{a_1})|a_1n\rangle \frac{1}{E_b^{(0)}-\varepsilon_{a_1}-\varepsilon_n} \langle n|e\alpha_\mu A_f^{\mu*}|a_2\rangle \right\}. \tag{27}$$

For the reducible part of the diagrams shown in Fig. 2(a) we have

$$\tau_{\gamma_f,b;a}^{(1a,\text{red})} = \frac{1}{2\pi i}\oint_{\Gamma_b} dE' \oint_{\Gamma_a} dE\, g_{\gamma_f,b;a}^{(1a,\text{red})}(E',E)$$

$$= \frac{1}{2\pi i}\oint_{\Gamma_b} dE' \oint_{\Gamma_a} dE \frac{1}{E'-E_b^{(0)}} \frac{1}{E-E_a^{(0)}} \left\{ \sum_P (-1)^P \left(\frac{i}{2\pi}\right)^3 \int_{-\infty}^{\infty} dp_2^0 dp_2'^0 \right.$$

$$\times \sum_n^{\varepsilon_{Pb_2}+\varepsilon_n=E_a^{(0)}} \left[\frac{1}{E-E_a^{(0)}} \left(\frac{1}{p_2'^0 - \varepsilon_{Pb_2}+i0} + \frac{1}{E-p_2'^0-\varepsilon_n+i0} \right) + \frac{1}{E'-p_2'^0-\varepsilon_{Pb_1}+i0} \frac{1}{E-p_2'^0-\varepsilon_n+i0} \right] \left(\frac{1}{p_2^0-\varepsilon_{a_2}+i0} \right.$$

$$\left. + \frac{1}{E-p_2^0-\varepsilon_{a_1}+i0} \right) \langle Pb_1|e\alpha_\mu A_f^{\mu*}|n\rangle \langle nPb_2|I(p_2'^0-p_2^0)|a_1a_2\rangle + \sum_P (-1)^P \left(\frac{i}{2\pi}\right)^3 \int_{-\infty}^{\infty} dp_1^0 dp_1'^0$$

$$\times \sum_n^{\varepsilon_{Pb_1}+\varepsilon_n=E_a^{(0)}} \left[\frac{1}{E-E_a^{(0)}} \left(\frac{1}{p_1'^0 - \varepsilon_{Pb_1}+i0} + \frac{1}{E-p_1'^0-\varepsilon_n+i0} \right) + \frac{1}{E'-p_1'^0-\varepsilon_{Pb_2}+i0} \frac{1}{E-p_1'^0-\varepsilon_n+i0} \right]$$

$$\left. \times \left(\frac{1}{p_1^0-\varepsilon_{a_1}+i0} + \frac{1}{E-p_1^0-\varepsilon_{a_2}+i0} \right) \langle Pb_2|e\alpha_\mu A_f^{\mu*}|n\rangle \langle Pb_1n|I(p_1'^0-p_1^0)|a_1a_2\rangle \right\}. \tag{28}$$

Calculating the residues at $E'=E_b^{(0)}$ and $E=E_a^{(0)}$ and using the identity (25), we obtain

$$\tau_{\gamma_f,b;a}^{(1a,\text{red})} = \sum_P (-1)^P \left\{ \sum_n^{\varepsilon_{Pb_2}+\varepsilon_n=E_a^{(0)}} \left[\frac{i}{2\pi} \int_{-\infty}^{\infty} dp_2^0 \frac{1}{(\varepsilon_{a_2}-p_2^0+i0)^2} \langle Pb_1|e\alpha_\mu A_f^{\mu*}|n\rangle \langle nPb_2|I(\varepsilon_{Pb_2}-p_2^0)|a_1a_2\rangle \right] \right.$$
$$\left. + \sum_n^{\varepsilon_{Pb_1}+\varepsilon_n=E_a^{(0)}} \left[\frac{i}{2\pi} \int_{-\infty}^{\infty} dp_1^0 \frac{1}{(\varepsilon_{a_1}-p_1^0+i0)^2} \langle Pb_2|e\alpha_\mu A_f^{\mu*}|n\rangle \langle Pb_1n|I(\varepsilon_{Pb_1}-p_1^0)|a_1a_2\rangle \right] \right\}. \tag{29}$$

We have assumed that the unperturbed states a and b are described by one-determinant wave functions (3) and (4). It implies that, in Eq. (29), we have to consider $(Pb_2,n)=(a_1,a_2)$ or (a_2,a_1) in first term and $(Pb_1,n)=(a_1,a_2)$ or (a_2,a_1) in second term. Therefore, the reducible part contributes only in the case when the states a and b have at least one common one-electron state. In what follows, we assume $a_1=b_1$ and $a_2 \neq b_2$. We obtain
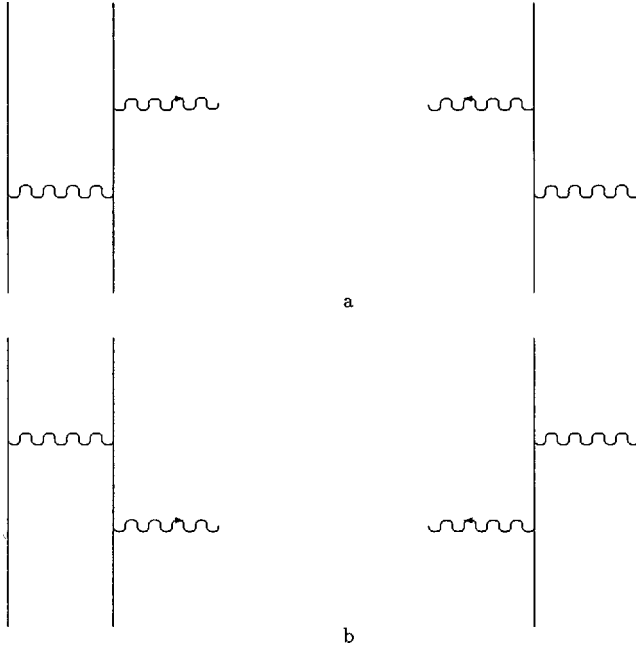
FIG. 2. The $1/Z$ interelectronic-interaction corrections to the photon emission by a heliumlike ion.

$$\tau_{\gamma_f,b;a}^{(1a,\text{red})} = \frac{i}{2\pi} \int_{-\infty}^{\infty} d\omega \langle b_2 | e\alpha_\mu A_f^{\mu*} | a_2 \rangle$$
$$\times \left(\frac{\langle a_1 a_2 | I(\omega) | a_1 a_2 \rangle}{(\omega - i0)^2} - \frac{\langle a_2 a_1 | I(\omega) | a_1 a_2 \rangle}{(\omega - \Delta_a - i0)^2} \right), \tag{30}$$

where $\Delta_a \equiv \varepsilon_{a_2} - \varepsilon_{a_1}$. A similar calculation of the reducible part of the diagrams shown in Fig. 2(b) gives

$$\tau_{\gamma_f,b;a}^{(1b,\text{red})} = \frac{i}{2\pi} \int_{-\infty}^{\infty} d\omega \langle b_2 | e\alpha_\mu A_f^{\mu*} | a_2 \rangle$$
$$\times \left(\frac{\langle b_1 b_2 | I(\omega) | b_1 b_2 \rangle}{(\omega - i0)^2} - \frac{\langle b_2 b_1 | I(\omega) | b_1 b_2 \rangle}{(\omega - \Delta_b - i0)^2} \right), \tag{31}$$

where $\Delta_b \equiv \varepsilon_{b_2} - \varepsilon_{b_1}$. The reducible contribution has to be considered together with second term in formula (18). Taking into account that
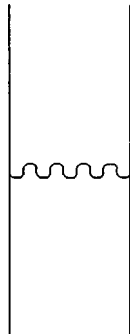

FIG. 3. One-photon exchange diagram.

TABLE I. The decay rates of the magnetic dipole transition $2\,^3S_1 \rightarrow 1\,^1S_0$ in units s^{-1}. The negative-continuum contribution $\Delta W_{e^+e^-}$ and the frequency-dependent correction ΔW_{freq} are expressed in percent with respect to the main term W. W_{tot} is the total decay rate value. The values presented in the upper part of the table were calculated in the Feynman gauge, whereas the results presented in the lower part were obtained using the Coulomb gauge.

Z	W	$\Delta W_{e^+e^-}$ (%)	ΔW_{freq} (%)	W_{tot}
30	8.9998×10^8	-0.043	-0.029	8.9933×10^8
50	1.7307×10^{11}	-0.08	-0.042	1.7286×10^{11}
70	5.9933×10^{12}	-0.132	-0.045	5.9827×10^{12}
90	9.4917×10^{13}	-0.205	-0.036	9.4688×10^{13}
30	9.0015×10^8	-0.05	-0.042	8.9933×10^8
50	1.7312×10^{11}	-0.09	-0.062	1.7286×10^{11}
70	5.9957×10^{12}	-0.145	-0.073	5.9827×10^{12}
90	9.4962×10^{13}	-0.218	-0.070	9.4688×10^{13}

$$\frac{1}{2\pi i} \oint_{\Gamma_a} dE\, g_{aa}^{(1)}(E)$$
$$= -\frac{i}{2\pi} \left[2 \int_{-\infty}^{\infty} dp_1'^0 \frac{1}{(p'^0 - \varepsilon_{a_1} - i0)^2} \right.$$
$$\times \langle a_1 a_2 | I(p_1'^0 - \varepsilon_{a_1}) | a_1 a_2 \rangle - \int_{-\infty}^{\infty} dp_1'^0 \frac{1}{(p_1'^0 - \varepsilon_{a_2} - i0)^2}$$
$$\times \langle a_2 a_1 | I(p_1'^0 - \varepsilon_{a_1}) | a_1 a_2 \rangle - \int_{-\infty}^{\infty} dp_1^0 \frac{1}{(p_1^0 - \varepsilon_{a_1} - i0)^2}$$
$$\times \langle a_2 a_1 | I(p_1^0 - \varepsilon_{a_2}) | a_1 a_2 \rangle \tag{32}$$

and a similar equation for the final state, one finds

TABLE II. The decay rates of the magnetic quadrupole transition $2\,^3P_2 \rightarrow 1\,^1S_0$ in units s^{-1}. The negative-continuum contribution $\Delta W_{e^+e^-}$ and the frequency-dependent correction ΔW_{freq} are expressed in percent with respect to the main term W. W_{tot} is the total decay rate value. The values presented in the upper part of the table were calculated in the Feynman gauge, whereas the results presented in the lower part were obtained using the Coulomb gauge.

Z	W	$\Delta W_{e^+e^-}$ (%)	ΔW_{freq} (%)	W_{tot}
30	2.1047×10^{10}	-0.0001	0.021	2.1051×10^{10}
50	1.3653×10^{12}	-0.001	0.038	1.3658×10^{12}
70	2.1470×10^{13}	-0.005	0.063	2.1483×10^{13}
90	1.7198×10^{14}	-0.017	0.097	1.7212×10^{14}
30	2.1051×10^{10}	-0.0001	0.001	2.1051×10^{10}
50	1.3658×10^{12}	-0.001	0.005	1.3658×10^{12}
70	2.1481×10^{13}	-0.005	0.014	2.1483×10^{13}
90	1.7209×10^{14}	-0.017	0.033	1.7212×10^{14}

TABLE III. The decay rates of the magnetic dipole transition $3\,^3S_1 \to 2\,^3S_1$, in units s^{-1}. The negative-continuum contribution $\Delta W_{e^+e^-}$ and the frequency-dependent correction ΔW_{freq} are expressed in percent with respect to the main term W. W_{tot} is the total decay rate value. The values presented in the upper part of the table were calculated in the Feynman gauge, whereas the results presented in the lower part were obtained using the Coulomb gauge.

Z	W	$\Delta W_{e^+e^-}$ (%)	ΔW_{freq} (%)	W_{tot}
30	6.1247×10^5	3.867	0.022	6.3628×10^5
50	1.3021×10^8	2.204	0.034	1.3313×10^8
70	4.9921×10^9	1.487	0.046	5.0686×10^9
90	9.0767×10^{10}	1.053	0.059	9.1776×10^{10}
30	6.1274×10^5	3.837	0.004	6.3628×10^5
50	1.3031×10^8	2.158	0.006	1.3313×10^8
70	4.9971×10^9	1.427	0.005	5.0686×10^9
90	9.0882×10^{10}	0.982	0.002	9.1776×10^{10}

$$
-\frac{1}{2}\oint_{\Gamma_b}dE'\oint_{\Gamma_a}dE\,g^{(0)}_{\gamma_f,b;a}(E',E)\left(\frac{1}{2\pi i}\oint_{\Gamma_a}dE\;g^{(1)}_{aa}(E)\right.
$$

$$
\left.+\frac{1}{2\pi i}\oint_{\Gamma_b}dE\;g^{(1)}_{bb}(E)\right)
$$

$$
=\frac{1}{2}\langle b_2|e\alpha_\mu A_f^{\mu*}|a_2\rangle\int_{-\infty}^{\infty}d\omega\left\{2\frac{\langle a_1a_2|I(\omega)|a_1a_2\rangle}{(\omega-i0)^2}\right.
$$

$$
+2\frac{\langle b_1b_2|I(\omega)|b_1b_2\rangle}{(\omega-i0)^2}-\langle a_2a_1|I(\omega)|a_1a_2\rangle
$$

$$
\times\left[\frac{1}{(\omega-\Delta_a-i0)^2}+\frac{1}{(\omega+\Delta_a-i0)^2}\right]-\langle b_2b_1|I(\omega)|b_1b_2\rangle
$$

$$
\left.\times\left[\frac{1}{(\omega-\Delta_b-i0)^2}+\frac{1}{(\omega+\Delta_b-i0)^2}\right]\right\}. \tag{33}
$$

Summing Eqs. (30), (31), and (33), we obtain for the total reducible contribution

$$
\tau^{(1,\text{red})}_{\gamma_f,b;a}=-\frac{1}{2}\langle b_2|e\alpha_\mu A_f^{\mu*}|a_2\rangle\frac{i}{2\pi}\int_{-\infty}^{\infty}d\omega\left\{\langle a_2a_1|I(\omega)|a_1a_2\rangle\right.
$$

$$
\times\left[\frac{1}{(\omega+\Delta_a+i0)^2}-\frac{1}{(\omega+\Delta_a-i0)^2}\right]
$$

$$
+\langle b_2b_1|I(\omega)|b_1b_2\rangle\left[\frac{1}{(\omega+\Delta_b+i0)^2}\right.
$$

$$
\left.\left.-\frac{1}{(\omega+\Delta_b-i0)^2}\right]\right\}. \tag{34}
$$

Here we have employed the symmetry property of the photon propagator: $I(\omega)=I(-\omega)$. Using the identity

$$
\frac{1}{(\omega+i0)^2}-\frac{1}{(\omega-i0)^2}=\frac{-2\pi}{i}\frac{d}{d\omega}\delta(\omega) \tag{35}
$$

and integrating by parts, we find

$$
\tau^{(1,\text{red})}_{\gamma_f,b;a}=\frac{1}{2}\langle b_2|e\alpha_\mu A_f^{\mu*}|a_2\rangle[\langle a_2a_1|I'(\Delta_a)|a_1a_2\rangle
$$

$$
+\langle b_2b_1|I'(\Delta_b)|b_1b_2\rangle], \tag{36}
$$

where $I'(\Delta)\equiv dI(\omega)/d\omega|_{\omega=\Delta}$ and it is implied that $a_1=b_1$. The total expression for $\tau^{(1)}_{\gamma_f,b;a}$ (in the case $a_1=b_1$) is given by the sum of equations (26), (27), and (36):

$$
\tau^{(1)}_{\gamma_f,b;a}=\tau^{(1a,\text{irred})}_{\gamma_f,b;a}+\tau^{(1b,\text{irred})}_{\gamma_f,b;a}+\tau^{(1,\text{red})}_{\gamma_f,b;a}. \tag{37}
$$

In addition to the interelectronic-interaction correction derived above, we must take into account the contribution originating from changing the photon energy in the zeroth-order transition probability (17) due to the interelectronic-interaction correction to the energies of the bound states a and b. It follows that the total interelectronic-interaction correction to the transition probability of first order in $1/Z$ is given by

$$
dW^{(1)}_{\gamma_f,b;a}=2\pi(k_f^0)^2 2\,\text{Re}\{\tau^{(0)*}_{\gamma_f,b;a}\tau^{(1)}_{\gamma_f,b;a}\}d\Omega_f+[\,dW^{(0)}_{\gamma_f,b;a}|_{k_f^0=E_a-E_b}
$$

$$
-\,dW^{(0)}_{\gamma_f,b;a}|_{k_f^0=E_a^{(0)}-E_b^{(0)}}],
$$

where E_a, E_b and $E_a^{(0)}$, $E_b^{(0)}$ are the energies of the bound

TABLE IV. The decay rate (s^{-1}) of the transition $2\,^3S_1 \to 1\,^1S_0$ calculated in this work is compared to the previous calculations and experiment. The experimental values and their error bars are given in second and fourth columns, respectively. In the last column the sum of our results and the QED corrections obtained in Ref. [13] are presented. In parentheses the uncertainties of the present calculations are indicated. Relative differences are calculated using experimental results as a reference.

Z	Expt.	Reference	Precision (%)	RMBPT (%) [2]	MCDF (%) [3]	Present (%)	Present +QED(%)
23	5.917×10^7	[14]	4.1	−0.1	−0.4	0.1	0.0(6)
26	2.083×10^8	[14]	12.5	−0.4	−0.7	−0.3	−0.4(5)
35	4.462×10^9	[15]	3.2	−2.3	−2.5	−2.1	−2.3(4)
36	5.848×10^9	[16]	1.3	−0.4	−0.6	−0.3	−0.5(4)
41	2.200×10^{10}	[17]	0.4	0.8	0.6	0.9	0.7(4)
47	8.969×10^{10}	[18]	1.8	1.3	1.2	1.5	1.2(2)
54	3.915×10^{11}	[19]	3.0	−1.8		−1.5	−2.0(2)

TABLE V. The decay rates (s^{-1}) of the transitions $2\,^3P_2 \rightarrow 1\,^1S_0$ and $3\,^3S_1 \rightarrow 2\,^3S_1$ obtained in this work are compared to the results obtained by RMBPT [4]. In parentheses the uncertainties of the present calculations are indicated.

| | $2\,^3P_2 \rightarrow 1\,^1S_0$ | | $3\,^3S_1 \rightarrow 2\,^3S_1$ | |
Z	This work	RMBPT	This work	RMBPT
30	$2.105(4) \times 10^{10}$	2.104×10^{10}	$6.36(5) \times 10^5$	6.35×10^5
50	$1.366(5) \times 10^{12}$	1.365×10^{12}	$1.331(8) \times 10^8$	1.33×10^8
70	$2.148(21) \times 10^{13}$	2.146×10^{13}	$5.07(5) \times 10^9$	5.06×10^9
90	$1.721(22) \times 10^{14}$	1.718×10^{14}	$9.18(12) \times 10^{10}$	9.15×10^{10}

states a, b with and without the interelectronic-interaction correction, respectively.

III. NUMERICAL RESULTS AND DISCUSSION

To evaluate the one-electron transition matrix elements, the explicit formulas given in Ref. [2] have been used. Infinite summations over the electron spectrum in Eqs. (26) and (27) have been performed by using the finite basis set method. Basis functions have been constructed from B splines by employing the procedure proposed in Ref. [11]. All the calculations have been carried out for the homogeneously charged sphere model of the nuclear charge distribution. The values for the nuclear radii were taken from Ref. [12].

In Tables I–III, we present our numerical results for the decay rates of the magnetic transitions $2\,^3S_1 \rightarrow 1\,^1S_0$, $2\,^3P_2 \rightarrow 1\,^1S_0$, and $3\,^3S_1 \rightarrow 2\,^3S_1$, respectively. The values presented in the upper and lower parts of the tables have been obtained in the Feynman and Coulomb gauges for the photon propagator, respectively. The transition energies used in the calculation were taken from Refs. [2,4]. The contribution due to the frequency dependence of the photon propagator ΔW_{freq} and the negative-continuum contribution $\Delta W_{e^+e^-}$ are given in these tables as well. It can be seen from the tables that the total values of the transition probabilities in the different gauges coincide with each other.

As one can see from Tables I and II, for the decays with $\Delta S \neq 0$, the frequency-dependent correction is of the same and even larger magnitude than the negative-continuum contribution. However, this is not the case for the $3\,^3S_1 \rightarrow 2\,^3S_1$ transition, where the correction ΔW_{freq} is small compared to the $\Delta W_{e^+e^-}$ term. The behavior of the negative-continuum correction as a function of the nuclear charge

number Z agrees well with the scaling ratio of the negative-to positive-energy contributions found in Ref. [4] for all the transitions under consideration.

In Tables IV and V, we compare our results with the previous calculations [2–4] that partially include the $1/Z^2$ and higher-order terms but do not account for the frequency-dependent contribution. In Table IV, the experimental data for the most precisely measured transition $2\,^3S_1 \rightarrow 1\,^1S_0$ are also presented. In the last column of this table our results are combined with the radiative corrections that are beyond the ones already included in the transition energy. These corrections were recently evaluated in Ref. [13] for the $2s_{1/2} \rightarrow 1s_{1/2}$ transition in hydrogenic ions for $Z \geqslant 50$. Since we consider high-Z two-electron ions, we can assume that the one-electron (hydrogenlike) approximation is sufficient to evaluate the related correction in He-like ions. We have extrapolated these data for $Z < 50$ and interpolated for $Z = 54$. The uncertainties due to the extrapolation of the radiative corrections and uncalculated $1/Z^2$ and higher-order terms are indicated in parentheses. In Table V, the comparison with the RMBPT calculations [4] is presented for the transitions $2\,^3P_2 \rightarrow 1\,^1S_0$ and $3\,^3S_1 \rightarrow 2\,^3S_1$. The uncertainties due to uncalculated radiative and higher-order interelectronic-interaction corrections are also indicated. From Tables I and IV, it can be seen that the frequency-dependent contribution is smaller than the current experimental accuracy.

In summary, we have presented a systematic quantum electrodynamic theory for the interelectronic-interaction corrections of first order in $1/Z$ to the transition probabilities in heliumlike ions. The numerical evaluation of these corrections to the magnetic transition probabilities has been performed and the equivalence of the Feynman and Coulomb gauges has been demonstrated. The results of the calculations performed have been compared with previous RMBPT calculations and with experiment.

[1] E. Lindroth and S. Salomonson, Phys. Rev. A **41**, 4659 (1990).

[2] W.R. Johnson, D.R. Plante, and J. Sapirstein, Adv. At., Mol., Opt. Phys. **35**, 255 (1995).

[3] P. Indelicato, Phys. Rev. Lett. **77**, 3323 (1996).

[4] A. Derevianko, I.M. Savukov, W.R. Johnson, and D.R. Plante, Phys. Rev. A **58**, 4453 (1998).

[5] G. Lach and K. Pachucki, Phys. Rev. A **64**, 042510 (2001).

[6] K. Pachucki, Phys. Rev. A **67**, 012504 (2003).

[7] V.M. Shabaev, Izv. Vuz. Fiz. **33**, 43 (1990) [Sov. Phys. J. **33**, 660 (1990)].

[8] V.M. Shabaev, Teor. Mat. Fiz. **82**, 83 (1990) [Theor. Math. Phys. **82**, 57 (1990)].

[9] V.M. Shabaev, Phys. Rev. A **50**, 4521 (1994).

[10] V.M. Shabaev, Phys. Rep. **356**, 119 (2002).

[11] W.R. Johnson, S.A. Blundell, and J. Sapirstein, Phys. Rev. A **37**, 307 (1988).

[12] G. Fricke, C. Bernhardt, K. Heilig, L.A. Schaller, L. Schellenberg, E.B. Shera, and C.W. de Jager, At. Data Nucl. Data Tables **60**, 177 (1995).

[13] J. Sapirstein, K. Pachucki, and K.T. Cheng, Phys. Rev. A **69**, 022113 (2004).

[14] H. Gould, R. Marrus, and P.J. Mohr, Phys. Rev. Lett. **33**, 676 (1974).

[15] R.W. Dunford, D.A. Church, C.J. Liu, H.G. Berry, M.L. Raphaelian, M. Hass, and L.J. Curtis, Phys. Rev. A **41**, 4109

[16] S. Cheng, R.W. Dunford, C.J. Liu, B.J. Zabransky, A.E. Livingston, and L.J. Curtis, Phys. Rev. A **49**, 2347 (1994).

[17] A. Simionovici, B.B. Birkett, R. Marrus, P. Charles, P. Indelicato, D.D. Dietrich, and K. Finlayson, Phys. Rev. A **49**, 3553 (1994).

[18] B.B. Birkett, J.P. Briand, P. Charles, D.D. Dietrich, K. Finlayson, P. Indelicato, D. Liesen, R. Marrus, and A. Simionovici, Phys. Rev. A **47**, R2454 (1993).

[19] R. Marrus, P. Charles, P. Indelicato, L. de Billy, C. Tazi, J.P. Briand, A. Simionovici, D.D. Dietrich, F. Bosch, and D. Liesen, Phys. Rev. A **39**, 3725 (1989).

(1990).